

Formation and Characterization of Silver Nanoparticle Composite with Poly(*p*-Br/F-phenylsilane)

Sung-Hee Roh^{1,*}, Ji Eun Noh², Hee-Gweon Woo^{2,*}, Myong-Shik Cho³, and Honglae Sohn⁴

¹Department of Chemical and Biochemical Engineering, Chosun University, Gwangju 501-759, Korea

²Department of Chemistry, Chonnam National University, Gwangju 500-757, Korea

³Gwangju Regional Food and Drug Administration, Gwangju 500-480, Korea

⁴Department of Chemistry, Chosun University, Gwangju 501-759, Korea

The one-pot production and structural characterization of composites of silver nanoparticles with poly(*p*-Br/F-phenylsilane), Br/F-PPS, have been performed. The conversion of Ag⁺ ions to stable Ag⁰ nanoparticles is mediated by the copolymer Br/F-PPS having both possibly reactive Si—H bonds in the polymer backbone and C—Br bonds in the substituents along with relatively inert C—F bonds. Transmission electron microscopy and field emission scanning electron microscopy analyses show the formation of the composites where silver nanoparticles (less than 30 nm of size) are well dispersed over the Br/F-PPS matrix. X-ray diffraction patterns are consistent with that for face-centered-cubic typed silver. The polymer solubility in toluene implies that the cleavage of C—Br bond and the Si—F dative bonding may not be occurred appreciably at ambient temperature. Nonetheless, thermogravimetric analysis data suggest that some sort of cross-linking could take place at high temperature. Most of the silver particles undergo macroscopic aggregation without Br/F-PPS, which indicates that the polysilane is necessary for stabilizing the silver nanoparticles.

Keywords: Composite, Cross-Linking, Polymeric Reducing Agent, Polymeric Stabilizer, Dehydrocoupling, Silver Nanoparticles, Copolysilane.

1. INTRODUCTION

Metals (Lewis acid) can be stabilized by the coordination of ligands (Lewis base) to form a complex. Polymer-protected, colloidal noble metal particles (i.e., Ag, Au, Pt) have received great attention because of their diverse applications in industry: e.g., in catalysis, electronics, green commodity, etc.^{1–5} In particular, suitable silver nanoparticles is important because bulk silver metal reveals the highest electrical and thermal conductivity among all metals, and the performance of silver metal in many applications may be significantly enhanced by processing bulk silver into nanosized silver.⁶ A few methods have been devoted to prepare different shaped silver nanostructures: (1) silver nanodisks, synthesized by using polystyrene mesospheres as templates⁷ and (2) silver nanowires prepared by using physical templates (e.g., carbon nanotubes,⁸ mesoporous materials,⁹ organic nanotubes arrays,¹⁰ etc.). Nonetheless, the high surface area of silver nanoparticles

have some disadvantages, i.e., the high inclinations of oxidative deterioration and aggregation when compared to the nanoparticles of gold and platinum metals. Thus, the protection of silver nanoparticles with proper polymer matrix should be absolutely necessary for proper applications.

An inorganic polymer with Si—Si bonding in the backbone, poly(*p*-Br/F-phenylsilane), (Br/F-PPS) was chosen as a stabilizer in this study. Inorganic polymers are generally known to have better optoelectronic and mechanical properties than organic polymers with main group element C in the backbone.¹¹ Hydrostannanes (or tin hydrides) and hydrogermanes (or germanium hydrides) in spite of their low bond energy (bond energy: 66 and 75 kcal/mol, respectively)¹² are not suitable because hydrostannanes are well known as toxic materials and hydrogermanes are quite expensive. In contrast, hydrosilanes (or silicon hydrides) are cheap and are reasonably not toxic. Thus, hydrosilanes (Si—H bond energy: 88 kcal/mol)¹² or polysilanes might be proper choice for

* Authors to whom correspondence should be addressed.

this experiment. In particular, Br/F-PPS is well suited for hosting noble metal nanoparticles for the following reasons:

(1) Hydrosilanes with backbone Si—H bonds, well-known reducing agents, have been successfully used for the generation of Pt, Pd, and Rh nanoparticles in the context of metal-catalyzed hydrosilylation of alkenes.¹³ Br/F-PPS with Si—H functionalities in the backbone can act as a reducing agent and thus can eliminate the need for an extra reducing agent.

(2) The Si—Si and C—Br bond (bond energy: 53 and 68 kcal/mol, respectively)¹² may have chance of being homolytically cleaved during the composite formation for inducing a chemical cross-linking of polymer matrix.

(3) Furthermore, although C—F bond may not be cleaved because of high bond energy (116 kcal/mol), F-PPS could undergo a physical cross-linking by a weak dative interaction between empty 3d orbitals of Si atoms (in backbone) and filled p orbitals of F (in substituent). In our approach, well-defined polyhydrosilanes are expected to act as reducing agents, as well as templates to control the size, stability, and solubility of nanoparticles ranging in diameter from less than 1 up to 30 nm.

(4) The glass-transition temperature (T_g) of Br/F-PPS is relatively lower than that of industrial organic polymer, such as polyvinyl chloride (PVC), polycarbonate (PC) or acrylonitrile-butadiene-styrene (ABS). This physical property has the advantage of making it easier to investigate the morphology of nanosilver/PPS composites as a function of their thermal treatment conditions at relatively lower fabrication temperatures.

Here we report the one-step preparation and structural characterization of silver nanoparticles/PPS composites. We also will discuss the synthesis parameters (including Br/F-PPS concentrations) influence the size and/or shape.

2. EXPERIMENTAL DETAILS

2.1. General Considerations

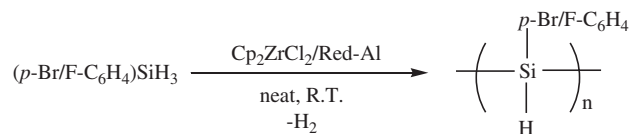
All reactions and manipulations were performed under ambient air atmosphere unless specified. Fourier-transform infrared (FT-IR) spectra of Br/F-PPS were acquired with a Nicolet 520P FT-IR spectrometer. Proton nuclear magnetic resonance (¹H NMR) spectra of Br/F-PPS were recorded on a Varian Gemini 300 spectrometer (operating at 300 MHz) using CDCl₃/CHCl₃ as a reference at 7.24 ppm downfield from tetramethylsilane (TMS). Gel permeation chromatography (GPC) was carried out on a Waters Millipore GPC liquid chromatograph. The calibrant (monodisperse polystyrene standard) and the sample were dissolved in tetrahydrofuran (THF) and separately eluted from an Ultrastyrigel GPC column series (sequence 500, 103, 104 Å columns). Molecular weights were extrapolated from the calibration curve derived from the polystyrene standard. Thermogravimetric analysis (TGA) of polymer sample was performed

on a Perkin Elmer 7 Series Thermal Analysis System under a nitrogen flow. Polymer sample was heated from 25 °C to 700 °C at a speed of 20 °C/min. Ceramic residue yield is reported as the percentage of the sample remaining after completion of the heating cycle. UV-Vis absorption spectra of samples were taken using a Hitachi U-3501 spectrometer. The transmission electron microscopy (TEM) images of the nanocomposites were obtained using a Tecnai F20 transmission electron microscope. Samples for TEM analysis were prepared by dip-coating a solution of a sample on formvar/carbon-film Cu grids (20 mesh, 3 mm). The average particle size and distribution were determined based on the measurement of at least 100 particles. The SEM image of the nanocomposite was obtained on a JSM-7500F field emission scanning electron microscopy (FE-SEM). X-ray diffraction (XRD) measurements were obtained with a D-Max-2400 diffractometer, equipped with graphite monochromatized Cu K_α radiation ($\lambda = 0.154$ nm). The total diameter (including the polysilane shell) of the silver nanoparticles was determined using dynamic light scattering (DLS) on a particle size analyzer (Malyern Zetasizer Nano) analysis. All the measurements were done at 25 °C. For the test, three replicate samples were used, and the average values were quoted. LiAlH₄, zirconocene (Cp₂ZrCl₂), Red-Al (Na[H₂Al(OCH₂CH₂OCH₃)₂]), and silver nitrate (AgNO₃) were purchased from Aldrich Chemical Co. and were used as received without further purification. (*p*-X-C₆H₄)Si(OEt)₃ (X = F, Br) was prepared by the controlled Grignard reaction of 1,4-dibromobenzene (and 1-fluoro-4-bromobenzene) with Si(OEt)₄. (*p*-X-C₆H₄)Si(OEt)₃ was then converted to (*p*-X-C₆H₄)SiH₃ with LiAlH₄ in diethyl ether solvent in good yield.

2.2. Dehydrocoupling of (*p*-Br/F-C₆H₄)SiH₃ Catalyzed by Cp₂ZrCl₂/Red-Al Combination

In a typical dehydrocoupling synthesis, (*p*-Br-C₆H₄)SiH₃ (1.55 g, 8.30 mM) and (*p*-F-C₆H₄)SiH₃ (0.12 g, 0.92 mM) were slowly added to a Schlenk flask containing Cp₂ZrCl₂ (54.0 mg, 0.18 mM) and Red-Al (56.0 μL, 0.18 mM; 3.40 M solution in toluene). The reaction mixture immediately turned light yellow, and the reaction medium became rapidly viscous with the vigorous evolution of hydrogen gas. The reaction mixture was allowed to stir under a stream of nitrogen for 24 hrs to reach the steady state of polymer molecular weight distribution. The catalyst was allowed to oxidize by exposure to the air, and then the mixture was dissolved in toluene. The solution was then passed rapidly through a Florisil column (100–200 mesh, 20 cm × 2 cm) under air atmosphere. The column was rinsed with 200 mL of toluene. The removal of volatiles at reduced pressure gave clear tacky product. The product was identified as Br/F-PPS by ¹H NMR, FT-IR, and GPC. FT-IR (film, KBr, cm⁻¹): 2111 ($\nu_{\text{Si—H}}$). ¹H NMR (CDCl₃, 300 MHz, δ ppm): 3.50–4.50 (br, SiH), 6.30–7.70 (br, C₆H₄). GPC $M_w = 2650$, $M_n = 2220$,

PDI (M_w/M_n) = 1.19. TGA residue yield = 45% (at 700 °C).



2.3. Synthesis of the Nanosilver/Br/F-PPS Composites

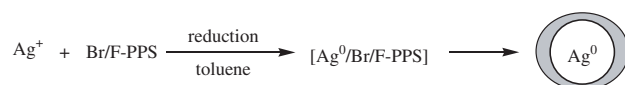
Br/F-PPS composite with silver nanoparticles were synthesized by reducing AgNO_3 in the presence of Br/F-PPS in toluene. Br/F-PPS (0.81 g, 4.60 mM) was dissolved in 50 mL of toluene, and AgNO_3 (0.131 g, 0.77 mM) was added (thus maintaining the weight ratio between AgNO_3 and Br/F-PPS approximately equal to 1:6) while stirring gently at room temperature under ambient atmosphere. The color of the reaction mixtures changed rapidly from light yellow to dark brown, indicating the formation of silver nanoparticles. Finally, the mixture was separated by ultracentrifugation. After collecting the deposit, washing with THF several times and vacuum-drying, the Ag/Br/F-PPS composite was acquired. TGA residue yield = 83% (at 700 °C). XRD, FE-SEM, and TEM analyses were performed on the composite sample.

3. RESULTS AND DISCUSSION

When a mixture of AgNO_3 in toluene is reduced in the presence of Br/F-PPS (Scheme 1), the color of the solution changes from pale yellow to dark brown due to the reduction of Ag^+ ions to Ag^0 nanoparticles. UV-Vis spectra (operating range 180–1000 nm; cuvette path length: 10 mm) were obtained to confirm the formation of silver nanoparticles.

Figure 1 shows the XRD patterns of the samples prepared by the reaction AgNO_3 with Br/F-PPS where Br/F-PPS serves as both structure-directing (stabilizing) agent and reducing agent. All diffraction peaks can be readily indexed to *fcc* (face-centered-cubic) silver with a calculated parameter $a = 4.09 \text{ \AA}$, which is in good agreement with the literature values (JCPDS 4-0783). The sharpness of the peaks indicates that the products are well crystallized.

TEM images (Figs. 2(a) and (b)) of the nanosilver/Br-PPS composites in Figure 2 show that they are of the randomly ramified nanostructure, composed of near-spherical nanoparticles with about 10–20 nm in diameter. The total diameter including the Br/F-PPS shell of the silver nanoparticle was $131.3 \pm 8.4 \text{ nm}$. SEM image (Fig. 2(c)) of the nanosilver/Br/F-PPS composite exhibits



Scheme 1. Preparation of nanosilver/Br/F-PPS composite.

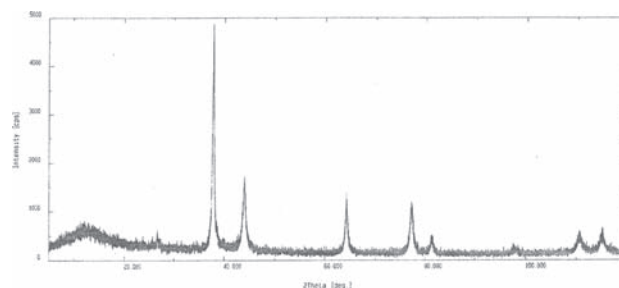


Figure 1. XRD pattern of the Ag/Br/F-PPS nanocomposites prepared by reacting AgNO_3 with Br/F-PPS.

silver nanoparticles well dispersed over Br/F-PPS matrix. Corresponding selected area electron diffraction (SAED) of the silver nanostructure shown in inset of Figure 2(d). The clear spots in Figure 2(d) (SAED of the silver nanostructures) indicate that these Ag nanoparticles are single crystals and can be indexed to (1, 1, 1), (2, 2, 2), and (3, 3, 1) reflections from *fcc* silver, and the zone axis projection is along.¹⁴

The ceramic residue yield of Br/F-PPS was enhanced from 45% to 85% after treating with AgNO_3 while that of PPS is 39%, indicating C—Br and C—F contribute to the increase of TGA ceramic yield by the small degree of cross-linking with C—Br bond hemolysis and F—Si dative bonding at high temperature, respectively. This fact suggests that the thermal stability of the polymer is improved due to the presence of silver as a nanofiller and a cross-linking agent at high temperature.

If decreasing the concentration of Br/F-PPS to one-third of the original one (thus maintaining the weight ratio between AgNO_3 and Br/F-PPS approximately equal to 1:2) and keeping other conditions constant, the bigger spherical nanoparticles are mainly obtained because of the increase of aggregation of silver nanoparticles. The TEM images (Fig. 3) of the sample show that they are of

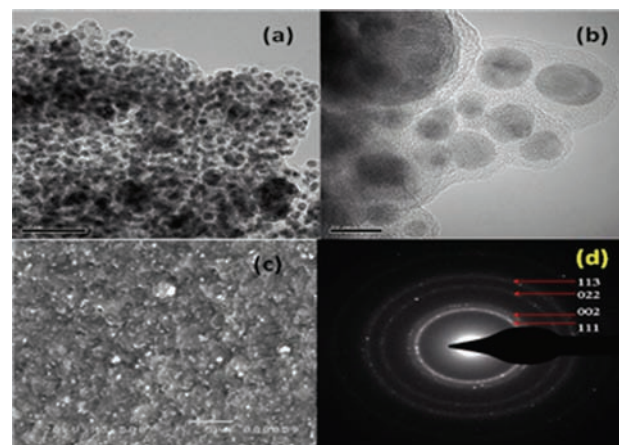


Figure 2. TEM images ((a) and (b)) and SEM image (c) of nano/Br/F-PPS nanocomposites. Inset of (d) shows the selected area electron diffraction patterns of the silver nanostructures.

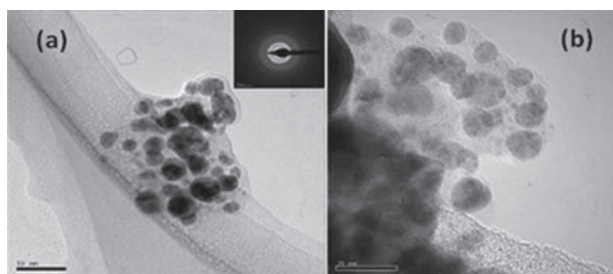


Figure 3. TEM images ((a) and (b)) of the bigger spherical silver nanoparticles. Inset of (a) shows the selected area electron diffraction patterns of the silver nanostructures.

the randomly ramified nanostructure, composed of near-spherical nanoparticles with about 15–30 nm in diameter.

The hydrophobic backbone and Si—H bonds of the polymers apparently induce the stabilization of the hydrophobic silver colloid particles, but also promote the agglutination of the primary polymer chains to a more complex, three-dimensionally functionalized structure. The reaction scheme for producing spherical nanoparticles involves the reduction of the soluble silver (+1) complex species, nucleation of metallic particles, and growth of the individual nuclei in the presence of a suitable reducing and stabilizing agent. The presence of Br/F-PPS is essential for preventing the coalescence of the nuclei during the growth step. Cross-linking was observed at high temperature as seen in the TGA analysis. The presence of this agent at the solid–liquid interface does not interfere with the silver diffusion-surface deposition process, and the particles thus can grow to a definite size. A series of extensive studies on the formation of nanocomposites of noble metal-group 14 compounds with various polymers such as inorganic, organic, and hybrid polymers are in progress. These results will be published elsewhere in due course.

4. CONCLUSION

A one-step conversion of Ag^+ ions to stable Ag^0 nanoparticles is made rapidly by a simple and mild Br/F-PPS-mediated reduction. PPS plays an important role in the

formation of the silver nanostructures, namely it provides lots of active sites for the coordination, nucleation, growth and serves as backbones for the assembly of the nanoparticles formed. Poly(*p*-Br/F-phenylsilane)s, Br/F-PPSs with Si—H functionalities also can act as a reducing agent and thus can eliminate the need for extra reducing agents which will be problematic to remove after reaction. The inorganic polymer, Br/F-PPS, apparently stabilizes the silver nanoparticles by preventing them from aggregating. The amount of Br/F-PPS added to the solution can affect the growth process of the silver nanoparticles. SEM and TEM analyses revealed that the particle dimension is nanometer scale.

Acknowledgment: This research was supported by the Global Research Laboratory (Grant Nos. K20903002024-12E0100-04010) through the National Research Foundation of Korea (NRF) funded by the Ministry of Science.

References and Notes

1. N. Toshima, T. Yonezawa, and K. Kushihashi, *J. Chem. Soc.* 89, 2537 (1993).
2. Y. Kim, J. Lee, and J. Yi, *J. Nanosci. Nanotechnol.* 8, 5090 (2008).
3. H. Hirai, H. Chawanya, and N. Toshima, *React. Polym.* 3, 127 (1985).
4. K. J. Lee, B. Lim, Y. H. Jeong, S. J. Hong, K. B. Lee, K. D. Kim, J. Kim, H. T. Kim, and Y. H. Choa, *J. Nanosci. Nanotechnol.* 8, 5090 (2008).
5. H. J. Kim, S. H. Choi, S. H. Oh, J. C. Woo, and I. K. Kim, *J. Nanosci. Nanotechnol.* 8, 4962 (2008).
6. Y. G. Sun and Y. N. Xia, *Adv. Mater.* 14, 833 (2002).
7. E. Hao, K. L. Kelly, J. T. Hupp, and G. C. Schatz, *J. Am. Chem. Soc.* 124, 15182 (2002).
8. A. Govindaraj, B. C. Satishkumar, M. Nath, and C. N. R. Rao, *Chem. Mater.* 12, 202 (2000).
9. W. Zhu, Y. Han, and L. An, *Microporous and Mesoporous Mater.* 80, 221 (2005).
10. B. H. Hong, S. C. Bae, C. W. Lee, S. Jeong, and K. S. Kim, *Science* 294, 348 (2001).
11. J. E. Marks, H. R. Allcock, and R. West, *Inorganic Polymers*, Prentice Hall, New Jersey (1990).
12. R. Walsh, *Acc. Chem. Res.* 14, 246 (1981).
13. L. N. Lewis, *Chem. Rev.* 93, 2693 (1993).
14. A. Govindaraj, B. C. Satishkumar, M. Nath, and C. N. R. Rao, *Chem. Mater.* 12, 202 (2002).

Received: 19 June 2013. Accepted: 13 November 2013.